Optimizing GPS Kinematic Accuracy by Employing the Kalman Filter Technique, the Case Study of Mecca - Medina Highway

Tarek A. Eldamaty
Civil Engineering Department, Umm Al-Qura University, College of Engineering and Architecture, Makkah, Saudi Arabia
tadamaty@uqu.edu.sa

Medhat M. Helal
Civil Engineering Department, Umm Al-Qura University, College of Engineering and Architecture, Makkah, Saudi Arabia
mmhelal@uqu.edu.sa (corresponding author)

Received: 10 February 2025 | Revised: 27 February 2025 | Accepted: 9 March 2025

 DOI: https://doi.org/10.48084/etasr.10528

ABSTRACT

This study presents an analysis of the feasibility of integrating a Kalman filter model with GPS kinematic data to improve position accuracy. The focus is on estimating the receiver's coordinates for a set of points using pseudo-range measurements from a single handheld GPS receiver. GPS signal errors compromise the accuracy of positioning, and a Kalman filter is utilized to improve the kinematic positioning of GPS points using a single-frequency I-COM GP 22 handheld receiver along a 180 km segment of the Mecca-Medina highway in Saudi Arabia to establish an accurate layer of the highway in a GIS system. A Kalman filter allowed characterizing noise sources and reducing their impact on the receiver's output. The core of the GPS-Kalman filter was a model that describes how the state vector evolves over time. As a recursive estimator, the Kalman filter provides the minimum covariance estimate of the state vector by processing and weighting measurements relative to the model's assumptions. The numerical results demonstrate that the RMS of the observed data before filtering was 4.2 m in the east direction and 3.7 m in the north direction. After applying the Kalman filter model, the RMS values decreased to 1.4 m in the east and 1.2 m in the north. The Kalman filter technique is a valuable tool for enhancing dynamic process analysis.

Keywords-GPS; kinematic measurements; Kalman filter; errors; position accuracy; navigation

I. INTRODUCTION

The Kalman Filter (KF) and the extended KF dynamics were introduced and derived in [1]. KF calculates the state estimate that minimizes the mean square error and is a linear, discrete-time, and finite-dimensional time-varying system. In [2], a KF data fusion technique was used to improve GPS positioning, where position and velocity were tracked using a basic motion model. The motion model used sensors that are frequently found in contemporary smartphones, while the raw data and a basic moving average filter were compared to assess the KF. In [3], an adaptively robust KF was proposed, with an adaptive factor to effectively control measurement errors. The position and velocity estimation error rates of the proposed GPS positioning system were tested, and the experimental results showed that the proposed method could provide a high-quality GPS positioning service. In [4], a unique robust Student's t-based KF was proposed to address the problem of a linear system with heavy-tailed process and measurement disturbances. In [5], the use of the received signal strength from the onboard communication module addressed the issue of continuous positioning and collision avoidance on UAVs in outdoor search scenarios. In [6], a weighted KF was used based on the variance estimation method to present a novel, fast, and precise GPS location system.

The GPS position can deteriorate from a few to ten meters due to several factors [6]. These sources of errors include atmospheric delays, ionospheric conditions, satellite, and receiver clock errors, multipath, and precision dilution. VHF/UHF lines may be used to convey errors, and users may use the corrections to pinpoint their positions with greater precision. The KF recursive method can be used to minimize these errors and produce a more precise approximation of the user's coordinates [7]. Precise point positioning is necessary to establish the base map of GIS layers [8].

GIS is a computer-based system that provides the following four sets of capabilities to handle georeferenced data: input, data management (data storage, maintenance, and retrieval), manipulation and analysis, and output [9]. GIS allows

interpreting and visualizing data in many ways that reveal relationships, patterns, and trends in the form of maps, globes, reports, and charts [10].

II. FUNDAMENTALS OF KALMAN FILTERING (KF)

The generic stochastic filtering problem involves using an observation process to iteratively estimate the present state of a random process. Over the past few decades, KF has been a common practice in surveying and geodetics, solving the estimation problem for a linear dynamic system with noisy observations [11].

A. Kinematic Model

The vehicle's motion and the dynamic noise that goes along with it are described by the kinematic model [12]. The linear system's dynamics are represented by the following first-order differential equation [6, 11]:

$$\xi'(\tau) = \varphi(\tau) + \omega(\tau) \quad (1)$$

where $\xi(\tau)$ is the system express vector that includes entirety parameters, $\varphi(\tau)$ is the dynamic matrix, and $\omega(\tau)$ is the random forcing matrix.

B. Linearized Equations

The linearized equations are built up in terms of a single KF model's loop cycle. The corresponding linearized dynamic model of (1) is described by the following relations:

$$\xi_{h+1} = \varphi_h + \omega_h \quad (2)$$

According to the linear connection, it is expected that the process's observations (measurements) take place at distinct times:

$$\zeta_h = \lambda_h \xi_h + \upsilon_h \quad (3)$$

where ξ_h is the process state vector at time τ, φ_h is a matrix relating $\xi(\tau)$ to $\xi(\tau+1)$, ω_h is a vector assumed to be a white (uncorrelated) sequence with a known covariance structure, ζ_h is the measurement vector at time τ, λ_h is a matrix giving the ideal (noiseless) relation between the measurements and the state vector at time τ and υ_h is the measurement error, assumed to be a sequence with known covariance structure and uncorrelated ω_h. The covariance matrices of ω_h and υ_h vector are given by:

$$E[\omega_h {\omega_i}^T] = Q_h \quad \text{only at} \quad i = h \quad (4)$$

$$E[\upsilon_h \upsilon_i^T] = R_h \quad \text{only at} \quad i = h \quad (5)$$

$$E[\omega_h {\upsilon_i}^T] = 0 \quad \text{for all} \quad h \text{ and } i \quad (6)$$

At this point, it is assumed that there is an initial estimate (prior estimate ξ_{h-} of the process at a specific time τ_h). It is also assumed that the error covariance matrix (ρ_{h-}) associated with the prior estimate is known. In many cases, the estimation problem is started with no prior measurements. Thus, in this case, the process mean is zero, the initial estimate is zero and the associated error covariance matrix is just the covariance matrix of ξ itself [13]. With the assumption of a prior estimate ξ_{h-}, the ζ_h measurements are used to improve the prior estimate according to:

$$\xi_{h+} = \xi_{h-} + \kappa_h(\zeta_h - \lambda_h \xi_{h-}) \quad (7)$$

where ξ_{h+} is the updated estimate and κ_h is the blending factor, which minimizes the mean square error and is called the Kalman gain. The state after measurement incorporation is generally accepted as the most optimal state in the filter since it is punctual and has the most recent measurement.

This equation can be used to calculate the covariance matrix associated with the optimal estimate, as updating the covariance for the subsequent state update comes after the measurement is considered.

$$\rho_h = (I - \kappa_h \lambda_h)\, \rho_{h-} \quad (8)$$

where I is the identity matrix and Kalman gain indicates how much the new measurement has improved the covariance.

The Kalman achieved is the outcome of an estimation completed at each measurement, based on the propagated covariance from the previous time ρ_{h-} and the measurement noise covariance R_h. The Kalman obtained can be calculated from the following equation:

$$\kappa_h = \rho_{h-} {\zeta_h}^T / \left(\lambda_h \rho_{h-} {\zeta_h}^T + R_h\right) \quad (9)$$

Although this equation appears complicated, a basic premise can help in understanding this gain calculation intuitively. Assume that the state and measurement are in the same coordinate form (so λ_h is the identity matrix) and the Kalman gain will be:

$$\kappa_h = \rho_{h-} / (\rho_{h-} + R_h) \quad (1)$$

For large uncertainty in the state model ρ_{h-} compared with the uncertainty in the measurement noise model R_h, Kalman gain applied to the new measurement is near unity. Finally, the update ξ_{h+} is easily projected ahead via the transition matrix through:

$$\xi_{(h+1)+} = \varphi_h \xi_{h+} + \omega_h \quad (11)$$

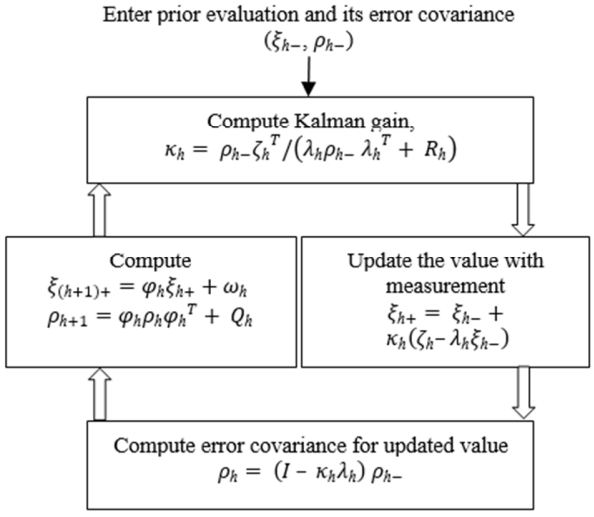

Fig. 1. KF model's loop.

C. Kalman Filter (KF) Model's Loop

Figure (1) illustrates the KF model's loop. It is evident that once the loop is started, it can go on forever.

III. METHODS

The primary goal was to determine whether it would be feasible to combine GPS measurements and the suggested KF model to increase position accuracy. A survey was carried out along the highway between Mecca and Medina. A 180 Km section of the road path was chosen. The receiver was installed in a compact vehicle that traveled at a steady pace. Using a GPS receiver, the location of pre-selected points and the vehicle's velocity were ascertained while traveling along the chosen route.

TABLE I. GPS NODE COORDINATES

Point ID	GPS coordinates before filtering		GPS coordinates after filtering		Map coordinates	
	East (m)	North (m)	East (m)	North (m)	East (m)	North (m)
P1	21542317	39778737	21542319	39778740	21542321	39778742
P2	21544538	39777744	21544540	39777747	21544541	39777748
P3	21547868	39777049	21547870	39777050	21547871	39777052
P4	21551761	39775962	21551758	39775959	21551757	39775958
P5	21554436	39775259	21554439	39775261	21554439	39775261
P6	21557488	39774660	21557491	39774663	21557492	39774665
P7	21561010	39773773	21561008	39773771	21561007	39773770
P8	21564888	39772870	21564891	39772872	21564892	39772874
P9	21568219	39772273	21568222	39772276	21568222	39772278
P10	21571550	39770586	21571550	39770586	21571551	39770587
P11	21574419	39766807	21574419	39766807	21574419	39766807
P12	21577746	39763025	21577749	39763027	21577748	39763028
P13	21581914	39759849	21581911	39759846	21581910	39759845
P14	21586068	39755862	21586071	39755865	21586072	39755867
P15	21589120	39752779	21589124	39752782	21589124	39752784
P16	21592457	39748512	21592455	39748509	21592453	39748507
P17	21594034	39747487	21594035	39747488	21594036	39747489
P18	21598501	39743192	21598503	39743195	21598505	39743197
P19	21603296	39735991	21603295	39735990	21603293	39735988
P20	21607758	39732894	21607760	39732896	21607762	39732898
P21	21612545	39729289	21612550	39729291	21612550	39729293
P22	21616058	39721393	21616060	39721395	21616061	39721396
P23	21619257	39716080	21619253	39716077	21619252	39716075
P24	21625000	39710242	21624998	39710239	21624997	39710238
P25	21628506	39703198	21628508	39703200	21628508	39703200
P26	21630737	39697016	21630741	39697019	21630742	39697021
P27	21631892	39688339	21631890	39688337	21631889	39688336
P28	21634446	39680443	21634444	39680441	21634442	39680439
P29	21636353	39673739	21636358	39673743	21636357	39673744
P30	21636677	39665335	21636676	39665333	21636676	39665333
P31	21637474	39658808	21637473	39658810	21637474	39658810
P32	21638275	39652290	21638271	39652288	21638272	39652287
P33	21643222	39647141	21643219	39647138	21643218	39647137
P34	21644811	39639922	21644812	39639926	21644814	39639927
P35	21647371	39632034	21647368	39632032	21647367	39632031

The GPS receiver was a five-channel one, model I-COM GP-22. When there is no signal interruption, the receiver's manufacturer specifications indicate an accuracy of ±10 m. The position was determined every 30 seconds while the receiver was continuously monitoring. In the World Geodetic System 1984 (WGS 84), the acquired coordinates were Cartesian (east, north). It is important to note that there were no notable obstacles or signal disruptions. After preparation, the acquired observations were fed into the suggested KF model to obtain the filtered position coordinates. Plotting the study highway's route both before and after filtering allowed for a graphic comparison between them, and each plot was then compared to the digital version of the route taken from a 1:5000 scale map.

IV. RESULTS AND DISCUSSION

The easting and northing coordinates were acquired using the WGS 84 reference data following the highway's right-hand traffic lane from Mecca to Medina. The reference map's projection was Universal Transverse Mercator (UTM), and its datum was also WGS 84. Table I shows the following:

- A pre-filtered sample of GPS node coordinates.
- Sample GPS node coordinates following filtering using the suggested KF model.
- The identical coordinates derived from the cited map at a scale of 1:5000.

As seen in Figure 2, the path is the actual path that was taken from the cited map.

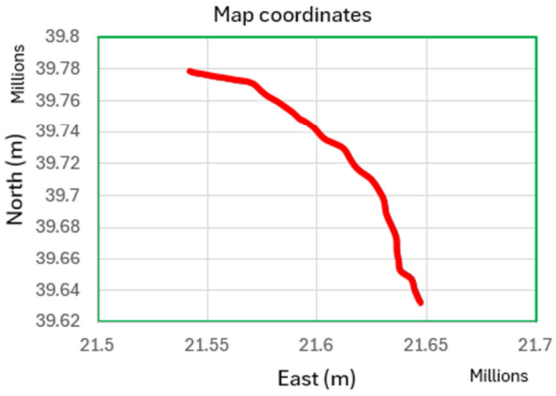

Fig. 2. The path from the reference map.

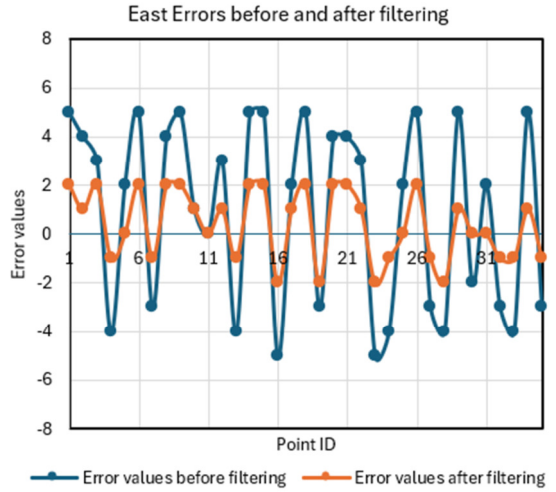

Fig. 3. The errors in the east direction before and after filtering.

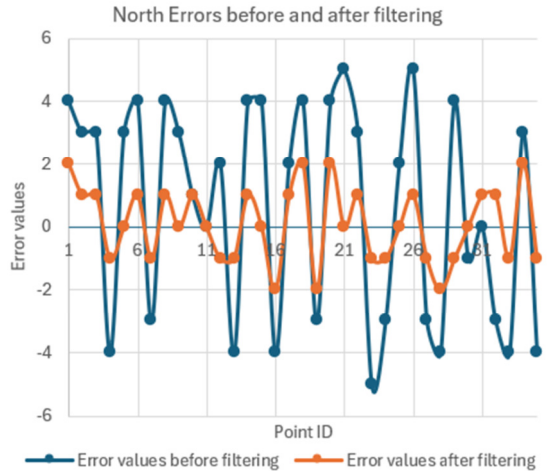

Fig. 4. The errors in the north direction before and after filtering.

TABLE II. ERROR VALUES BEFORE AND AFTER FILTERING

Point ID	Error values before filtering		Error values after filtering	
	ΔEb (m)	ΔNb (m)	ΔEa (m)	ΔNa (m)
P1	4	5	2	2
P2	3	4	1	1
P3	3	3	1	2
P4	-4	-4	-1	-1
P5	3	2	0	0
P6	4	5	1	2
P7	-3	-3	-1	-1
P8	4	4	1	2
P9	3	5	0	2
P10	1	1	1	1
P11	0	0	0	0
P12	2	3	-1	1
P13	-4	-4	-1	-1
P14	4	5	1	2
P15	4	5	0	2
P16	-4	-5	-2	-2
P17	2	2	1	1
P18	4	5	2	2
P19	-3	-3	-2	-2
P20	4	4	2	2
P21	5	4	0	2
P22	3	3	1	1
P23	-5	-5	-1	-2
P24	-3	-4	-1	-1
P25	2	2	0	0
P26	5	5	1	2
P27	-3	-3	-1	-1
P28	-4	-4	-2	-2
P29	4	5	-1	1
P30	-1	-2	0	0
P31	0	2	1	0
P32	-3	-3	1	-1
P33	-4	-4	-1	-1
P34	3	5	2	1
P35	-4	-3	-1	-1

Some geometric characteristics of the road were not precisely mapped because of the low observation rate. Errors in the geometric properties of the path may be caused by the GPS sample rate. Conventional factors such as atmospheric effect, orbit accuracy, pseudo-range resolution, and dynamic effect were among the other possible sources of inaccuracies. An additional cause of error is the path's digitization from the original map.

By subtracting the coordinates of the observation points before and after filtering from the coordinates of the reference map, the errors in the east and north directions were calculated for every point before and after filtering. Table II shows the error values. According to the numerical results, the RMS of the observed coordinates before filtering was 3.7 m in the North direction and 4.2 m in the east. After filtering, the RMS of the observed coordinates dropped to 1.4 m in the east direction and 1.2 m in the north direction. Figures 3 and 4 show errors in the east and north directions before and after filtering. The accuracy of GPS kinematic measurements was improved by the KF model, as evidenced by the decrease in errors in both the east and north directions.

V. CONCLUSION

Based on the developed KF model, GPS kinematic observations, and the points examined in this study, it is worth to conclude the following:

- It is evident that the KF significantly increases the precision of GPS data in kinematic positioning techniques and unquestionably produces superior outcomes.
- Noise warps GPS kinematic measurement, resulting in computation errors. Errors in the ionospheric corrections and system dynamics that were not considered during the measurement process are included in this noise. To reduce the impact of noise sources on the intended measurements, the KF approach can be used to characterize them.
- Maps with a scale of 1:10000 or less might be updated using the GPS absolute kinematic mode. Additionally, it can be used to create special-purpose maps, such as emergency maps and tourist guides, that do not require a high level of accuracy.

Future studies will focus on the development and analysis of a fuzzy extended KF. Additionally, future research can focus on ways to enhance the filter's initial values and the covariance matrices.

REFERENCES

[1] M. I. Ribeiro, "Kalman and Extended Kalman Filters: Concept, Derivation and Properties," Institute for Systems and Robotics, Lisboa, Portugal, Feb. 2004.

[2] M. Eliasson, "A Kalman Filter Approach to Reduce Position Error for Pedestrian Applications in Areas of Bad GPS Reception," B.S. Thesis, UMEA University, 2014.

[3] X. Wang and M. Liang, "GPS Positioning Method Based on Kalman Filtering," in *2018 International Conference on Robots & Intelligent System (ICRIS)*, Changsha, China, May 2018, pp. 77–80, https://doi.org/10.1109/ICRIS.2018.00028.

[4] G. Jia, N. Li, M. Bai, and Y. Zhang, "A Novel Student's t-based Kalman Filter with Colored Measurement Noise," *Circuits, Systems, and Signal Processing*, vol. 39, no. 8, pp. 4225–4242, Aug. 2020, https://doi.org/10.1007/s00034-020-01361-6.

[5] C. Luo, S. I. McClean, G. Parr, L. Teacy, and R. De Nardi, "UAV Position Estimation and Collision Avoidance Using the Extended Kalman Filter," *IEEE Transactions on Vehicular Technology*, vol. 62,

no. 6, pp. 2749–2762, Jul. 2013, https://doi.org/10.1109/TVT.2013.2243480.

[6] S. Shokri, N. Rahemi, and M. R. Mosavi, "Improving GPS positioning accuracy using weighted Kalman Filter and variance estimation methods," *CEAS Aeronautical Journal*, vol. 11, no. 2, pp. 515–527, Jun. 2020, https://doi.org/10.1007/s13272-019-00433-x.

[7] W. Zhao, S. Khanafseh, and B. Pervan, "Adaptive Multiple-Model Kalman Filter for GNSS Carrier Phase and Frequency Estimation Through Wideband Interference," *NAVIGATION: Journal of the Institute of Navigation*, vol. 71, no. 2, 2024, https://doi.org/10.33012/navi.646.

[8] X.-B. Jin, W. Chen, H.-J. Ma, J.-L. Kong, T.-L. Su, and Y.-T. Bai, "Parameter-Free State Estimation Based on Kalman Filter with Attention Learning for GPS Tracking in Autonomous Driving System," *Sensors*, vol. 23, no. 20, Oct. 2023, Art. no. 8650, https://doi.org/10.3390/s23208650.

[9] T. Eldamaty, A. G. Ahmed, and M. M. Helal, "GIS-Based Multi Criteria Analysis for Solar Power Plant Site Selection Support in Mecca," *Engineering, Technology & Applied Science Research*, vol. 13, no. 3, pp. 10963–10968, Jun. 2023, https://doi.org/10.48084/etasr.5927.

[10] M. M. Helal and T. A. Eldamaty, "Urban Development Analysis using GIS and Remote Sensing. The Case Study of Makkah City," *Engineering, Technology & Applied Science Research*, vol. 14, no. 3, pp. 13864–13869, Jun. 2024, https://doi.org/10.48084/etasr.7019.

[11] M. S. Grewal and A. P. Andrews, *Kalman Filtering: Theory and Practice with MATLAB*, 4th ed. Wiley, 2014.

[12] N. Ashok Kumar, Ch. Suresh, and G. Sasibhushana Rao, "Extended Kalman Filter for GPS Receiver Position Estimation," in *Intelligent Engineering Informatics*, 2018, pp. 481–488, https://doi.org/10.1007/978-981-10-7566-7_47.

[13] L. Bagadi, G. S. Rao, and N. Ashok Kumar, "Firefly, Teaching Learning Based Optimization and Kalman Filter Methods for GPS Receiver Position Estimation," *Procedia Computer Science*, vol. 143, pp. 892–898, Jan. 2018, https://doi.org/10.1016/j.procs.2018.10.365.